The Electronic Structure of Beryllium Chains

Ahmad W. Huran, Nadia Ben Amor, Stefano Evangelisti, Sophie Hoyau, Thierry Leininger, Véronique Brumas

The Electronic Structure of Beryllium Chains

Ahmad W. Huran,[†,‡] Nadia Ben Amor,[‡] Stefano Evangelisti,[*,‡] Sophie Hoyau,[‡]

Thierry Leininger,[‡] and Véronique Brumas[¶]

†*Institut für Physik, Martin-Luther-Universität Halle-Wittenberg,*

D-06120 Halle (Saale), Germany

‡*Laboratoire de Chimie et Physique Quantiques,*

Université de Toulouse et CNRS,

118, Route de Narbonne, F-31062 Toulouse Cedex - France

¶*SIMAD, Université de Toulouse,*

118, Route de Narbonne, F-31062 Toulouse Cedex - France

E-mail: stefano.evangelisti@irsamc.ups-tlse.fr

Abstract

We present an *ab initio* theoretical study of quasi one-dimensional beryllium chains, Be_N, from an electronic structure perspective for N=3, 4,..., 12. In particular, linear and cyclic systems have been compared by using high-quality Coupled-Cluster formalism. Both linear and cyclic species have been found to be local minima on the corresponding Potential-Energy Surface, for all the considered values of N. The linear geometry is the most stable one only in the case of Be_4. Several indicators (energy gap, position spread tensor, locality of the molecular orbitals) clearly show that both linear and cyclic 1D structures, unlike 3D bulk beryllium, have a covalent insulating nature.

Introduction

The interest in atomically-thin linear surface-deposited structures has experienced huge growth in the last years. This growth was driven, for the most part, by the possibility of synthesizing one-dimensional electron systems at stepped surfaces.[1–5] These systems exhibit a common characteristic, namely the presence of edge orbitals, which correspond to what Tamm and Shockley introduced long ago as "surface states" in a one-electron picture.[6] The edge effects were predicted in graphene-based nanoribbons and nanodots,[7,8] that can give rise to a wide spectrum of interesting electric and magnetic phenomena.[9] These states, in one-dimensional setting, are referred to as "end states", the presence of which has been observed, for e.g., in one-dimensional chains of self-assembled gold atoms on silicon surfaces.[5]

Ab initio theoretical treatment of linear beryllium chains, close to equilibrium configurations, predicted the existence of two edge orbitals localized at the extremities of the chains.[10] These edge orbitals are partially filled, and lead to two low-lying quasi-degenerate states, namely, $^1\Sigma_g$ and $^3\Sigma_u$. The energy difference between the singlet ground state and the triplet state presents an exponential decay with increased length of the atomic chain.

Recently, a multitude of interesting effects and features exhibited by beryllium in different chemical environments have been theoretically predicted by Yáñez and coworkers. The formation of the so-called *beryllium bonds* between a Lewis base and a beryllium Lewis acid[11] was found to act as a modulator of intra-molecular interactions,[12] and as the driver of spontaneous radical formation.[13] Be-Be bonds on the other hand were proposed as possible moiety to trap anions utilizing the electron deficiency of the bond in what is known as *beryllium-based anion sponges*.[14,15] A new kind of Be-Be bonding was also predicted, namely a one electron Be-Be bond of a hybrid character dominated by the contribution of s orbitals.[16] Versatility of Be-based species extends well beyond small molecular structures and has spurred interest in the context of linear surface-deposited atomic chains, as it serves as a

prototypical subject for studying such chains. Linear beryllium chains have been extensively investigated by our group.[10,17–21] Because of the presence of unpaired electrons, unsaturated linear chains, would be certainly highly reactive. However, the terminal edge orbitals in a Be_N chain can be saturated by means of hydrogen atoms, finally obtaining a linear HBe_NH chain. Indeed, HBe_2H clusters have been observed in beryllium vapors by Tagues and Andrews.[22] Another possibility of getting a saturated species is by wrapping the chain into a ring, thus creating a topologically closed structure.[23–25] Notice that, although a ring is, strictly speaking, a 2-Dimensional (2D) system, its local topology has a close similarity to the 1-Dimensional (1D) chains. For this reason, both structures are considered as quasi-1D ones.

In this work, we studied the electronic structure of open (linear) and closed (cyclic) Be_N clusters, where N in any integer number ranging from 3 to 12. We optimized the geometry of both linear and cyclic chains by using a high-quality Coupled-Cluster (CC) formalism.

on the Potential Energy Surface (PES) for each structure. An important point that is addressed in this work concerns the nature of the Be-Be bond at equilibrium distance. Bulk 3D beryllium is a metal, and it is often said that the chains are quasi-1D metallic systems. Such an opinion can even be found, for example, in an article of one of the authors of the present paper.[26] In order to investigate this point, we studied the behavior of the Total-Position Spread (TPS) tensor as a function of the system size. Indeed, it has been shown by Resta and co-workers that the value of the TPS per-electron, or "Localization Tensor",[27–30] tends toward a finite quantity if the system is an insulator, while it diverges in the case of metals. For this reason, we computed the eigenvalues of the spread tensor for both types of chains.

The body of the article is structured as follows. Firstly, we consider beryllium chains from an electronic structure perspective. The case of linear and cyclic geometries will be compared. Then the theoretical framework of the investigation is given, and the details concerning the used computational techniques are described. The results are presented and

discussed thereafter: the symmetry and the canonical and localized orbitals of these systems are considered, and the Highest Occupied Molecular Orbital-Lowest Unoccupied Molecular Orbital (HOMO-LUMO) energy gaps discussed. Subsequently, results on the optimized geometries, harmonic frequencies, total energies and their extrapolation in the limit of infinite-length chains as well as the behavior of the TPS tensor are presented. Finally, we close by summarizing our main results and give concluding remarks.

Electronic Structure

Beryllium has four electrons in the isolated atom, and a closed-shell electronic configuration, $1s^2 2s^2$. This leads to an electronic structure somewhat resembling that of a rare gas. Beryllium exhibits an Ionization Potential (IP) that is larger than the IP of its period successor, a relatively infrequent behavior in the Periodic Table, that beryllium shares with other Alkaline-Earth metals.

With only two valence electrons, beryllium is found in molecular moieties of co-linear geometrical configurations, for e.g., the well known case of beryllium hydride (BeH_2), and the less studied, $Be_N H_2$ linear structures.[22]

Consider a linear arrangement of N beryllium atoms that, for simplicity, defines the z axis of our reference Cartesian coordinate system. We assume a $D_{\infty h}$ as the symmetry point group of the chain, to be verified, and label the orbitals by g and u according to their character under the inversion symmetry operation.

For a qualitative description of the electronic structure of the systems at hand it is enough to consider σ valence orbitals, as the role of π valence orbitals can be neglected due to their relatively high energies. For a chain made of N Be atoms, the total number of valence

electrons is $2N$. $2N-2$ of these electrons are accommodated in the $N-1$ σ-bonds formed from the inner sp_z hybrids along the chain. The outer sp_z hybrids combine to form two edge orbitals a σ_g, and a σ_u hosting the remaining two valence electrons. In terms of these two symmetry-adapted orbitals, the lowest energy configurations of the two edge electrons are $\frac{1}{\sqrt{2}}(\sigma_g\bar{\sigma}_g - \sigma_u\bar{\sigma}_u)$, and $\frac{1}{\sqrt{2}}(\sigma_g\bar{\sigma}_u + \sigma_u\bar{\sigma}_g)$, yielding a singlet $^1\Sigma_g$ and a triplet $^3\Sigma_u$ state, respectively. Due to the large separation between the edge sp_z hybrids, the aforementioned states are quasi-degenerate.

We consider now the total energy of both linear and cyclic systems. In the case of linear systems, we have shown[17–20] that the total energy can be expressed as:

$$E_{\text{linear}}(N) = \overline{E}_{\text{ST}}(N) = (N-1)E_{\text{Be-Be}} + E_{\text{Be}\cdot} \tag{1}$$

where $\overline{E}_{ST}$ indicates the mean singlet-triplet energy, $E_{\text{Be-Be}}$ is the energy of a Be atom having two Be-Be bond, while $E_{Be\cdot}$ is the energy associated to the terminal edge electrons. In practice, for large systems, the singlet and the triplet are degenerate, so one can extract the total energy from single-reference calculations on the triplet. Notice that by using this definition the energies associated to the inner core electrons are absorbed in the bond or edge energy definition. The total energy per Be atom can be rewritten as

$$E_{\text{linear}}(N)/N = E_{\text{Be-Be}} + \frac{1}{N}(E_{\text{Be}\cdot} - E_{\text{Be-Be}}) \tag{2}$$

This means that the energy per atom is a *linear* function of $1/N$, N being the number of beryllium atoms. The limit for $N \to \infty$ gives the energy per atom of the infinite chain, while the (formal) extrapolation of the curve to the value $N = 1$ gives the value of the $E_{\text{Be}\cdot}$ parameter.

In the case of cyclic systems, on the other hand, no terminal effects are present. In turn,

in this case, the presence of a strain energy must be considered. This is due to the fact that the two bonds on each beryllium atom, -Be-, form an angle smaller than π, which is the ideal one for the *sp* hybridization of beryllium atoms. In the case of a regular ring containing N atoms, the difference between the ideal angle π and the actual one is given by $\theta = 2\pi/N$. For small deformations from the ideal local geometry, the strain energy is expected to be a quadratic function of the deformation. In other words, for small values of θ (which means in the limit of long chains), the strain energy is expected to be a quadratic function of θ. Therefore, the total energy per beryllium atom will become

$$E_{\rm cyclic}(N)/N = E_{\rm Be-Be} + \frac{1}{N^2} E_{\hat{\rm Be}} \tag{3}$$

In this expression, $E_{\rm Be-Be}$ is the Be-Be bond energy, as in equation (2), while $E_{\hat{\rm Be}}$ represents the strain energy. Therefore, for cyclic chains, the total energy per atom is expected to be a *quadratic* function of $1/N$. As for the case of linear systems, limit for $N \to \infty$ gives the energy per atom of the infinite chain, while the line slope gives the $E_{\hat{\rm Be}}$ parameter. If the present analysis is correct, the parameter $E_{\rm Be-Be}$ should be exactly the same in the two energy expressions, eq.s (2) and (3). Notice that in these equations the parameters $E_{\rm Be-Be}$ and $E_{\rm Be\cdot}$ include also the large core energy associated to the $1s$ electrons.

In this work we are particularly interested in comparing linear and cyclic systems up to relatively long chains (N=12). This means that the use of high-quality *size-consistent* methods is particularly appropriate. With this respect, the Coupled-Cluster (CC) formalism is certainly the best tool nowadays available in Quantum Chemistry. However, CC formalism is presently restricted essentially to the treatment of closed-shell systems. This is not a problem for the treatment of cyclic chains, due to the single-reference nature of their ground state. Linear chains, on the other hand, have an open-shell singlet ground state, whose description is highly problematic at CC level. In the course of our previous investigations, however, we have shown that the single-reference first excited triplet is quasi degenerate with

the ground state. Their energy split, in fact, decreases exponentially as a function of the number of atoms in the chain, and can be safely neglected in energetic considerations except for the shortest chains for which the triplet is preferred. In the present investigation, in order to apply a high-quality Coupled-Cluster formalism to the study of the systems, we made the choice of studying the singlet ground state of cyclic chains and the triplet first-excited state in the case of linear chains.

Computational Details

Quasi-1D systems are the linear and cyclic chains. The linear chains have a $D_{\infty h}$ symmetry, while cyclic ones have D_{nh}, where N is the number of Be atoms. These symmetries have been checked *a posteriori* by means of a frequency calculation, as described in the following section. However, since most *ab initio* packages can only handle abelian groups, the actual calculations were carried out considering the largest abelian subgroup corresponding to the system at hand. This is the D_{2h} subgroup for linear and even cyclic chains, while odd cyclic chains were studied in the C_{2v} subgroup.

Crystalline metallic beryllium has a Hexagonal Close-Packing structure. In order to confirm the non-metallic nature of the Be-Be bonds in 1D structures, it is instructive to consider also three-dimensional (3D) clusters. Since Hexagonal Close-Packing (HCP) arrangements of weakly interacting atoms are often quasi-degenerate with Face-Centered Cubic (FCC) structures, we considered highly symmetric clusters as fragments of these crystal structures. The structures we chose are the tetrahedral Be_4 structure (T_d symmetry), and two isomers of Be_{13}: the icosahedral structure (I_h symmetry, which can be seen as a fragment of a FCC crystal), and a D_{3h} structure which is the seed of a HCP crystal. At HF level, Be_4 has a closed-shell ground state, and do not create particular difficulties. The two forms of Be_{13}, on the other hand, have open-shell ground states that require some caution. In particular FCC

Be_{13}, has a triply-degenerate HOMO manifold hosting four electrons, and it is not possible to have a neutral non broken-symmetry wavefunction. For this reason, we also considered the two ionic undistorted structures that are closest to the neutral one, *i.e.* the quartet Be_{13}^{+} and the singlet Be_{13}^{2-}. FCC Be_{13}, on the other hand, has a doubly degenerate HOMO pair containing two electrons, and we considered therefore the triplet lowest state.

The ANO-type basis set optimized by Widmark and co-workers was chosen for the atomic orbitals,[31] adopting the largest contraction recommended by the authors. We performed Restricted Hartree-Fock Self Consistent Field (RHF-SCF) and Complete Active Space SCF (CAS-SCF) calculations for the singlet ground state of cyclic system, and the triplet lowest state of diradical linear chains. Geometries have also been optimized at Coupled-Cluster level restricted to Single and Double excitations (CCSD). Finally, the contribution of triple excitations was taken into account at a perturbative level by performing a CCSD(T) calculation at the CCSD optimized geometry. The harmonic frequencies were evaluated numerically at the SCF and CCSD levels. All CC calculations were performed with doubly occupied RHF-frozen $1s$ orbitals.

Finally, we note that all the calculations reported in this work were carried out using the MOLPRO package.[32] In particular, we performed RHF-SCF, CAS-SCF, CCSD,[33] and CCSD(T)[34] calculations with the corresponding MOLPRO sections. Geometry optimizations were obtained through the rational-function approach and the geometry DIIS algorithm.[35]

Results and Discussion

We discuss here the behavior of the singlet ground state of cyclic Be_N chains and the first excited triplet state of linear chains containing N Be atoms for values of N ranging from 3 to 12. Geometries were optimized at CCSD level (see Tables S1 and S2 in the Supplementary Information), and single-point calculations at the CCSD optimized geometries were performed at CCSD(T) level (Tables S3, and S4).

Linear-Chain Symmetry

The symmetry group of the linear chains Be_N is $D_{\infty h}$. The different equilibrium-bond-lengths of linear structures coincide up to few percents. The symmetry of the valence occupied orbitals for even chains ($N = 2m$) are, in ascending energy order, σ_g, σ_u, σ_g,... The two singly occupied molecular orbital (SOMO) have σ_u and σ_g symmetry and become quasi-degenerate orbitals for long chains. At CAS-SCF level, the two orbitals have very close occupations in the ground state singlet, $1^1\Sigma_g^+$. The lowest triplet state $1^3\Sigma_u^+$ is quasi degenerate with the ground state, and in this case the occupation numbers of the quasi-degenerate frontier orbitals are exactly those obtained at CAS(2/2) level.

Cyclic-Chain Symmetry

It turned out that the cyclic minima have D_{nh} symmetry, which means that the N atoms occupy the vertices of a regular polygon having N sides. We assume the molecule is placed on the xy plane, with the yz symmetry plane containing at least one atom. The symmetry of the valence occupied orbitals for even chains ($N = 2m$) are, in ascending energy order, a_{1g}, e_{1u}, e_{2g}, e_{3u},... The highest orbital has either b_{2g} or b_{2u} symmetry, for $N = 4k$ or $N = 4k+2$, respectively. Odd-N chains, on the other hand, ($N = 2m + 1$) have orbitals with symmetry a'_1, e'_1, e'_2,..., e'_m. This fact has important implications on the HOMO energies. In order to see

this, it is convenient to consider a Hückel model that involves the bonding orbitals between two adjacent atoms only. As usual, we assume a β value < 0 for the hopping integral between two adjacent orbitals (its actual value is arbitrary), while the monocentric α integral does not play any role, and can be put equal to zero. All the resulting orbitals will be doubly occupied, so this model is not able to describe any excitation. Nevertheless, it can give some useful information on the Highest Occupied Molecular Orbital (HOMO) structure. In fact, in the case of even-N cyclic chains, the HOMO is a non degenerate orbital. In the Hückel model, its energy has a constant value of -2β. The HOMO in odd cyclic chains is given by a pair of degenerate orbitals, whose Hückel energy is given by $-2\beta\cos(\pi/N)$. The two different behaviors are illustrated in Figure 1, where the orbital energies for the two cases of C_5H_5 and C_6H_6 are reported.

Canonical and local orbitals

In Figure 2a, some of the ROHF valence orbitals are shown, for a linear chain of intermediate length (Be_6) at the equilibrium geometry. The five doubly occupied canonical orbitals are different bonding combinations of Be-Be sp_z hybrid orbitals. The singly occupied edge orbitals are hybrid sp_z orbitals pointing towards the outer part of the chain.

Local orbitals have been obtained by a unitary transformation performed on the ROHF canonical orbitals for the case of $N = 6$, with the DOLO code.[36]

In Figure 3, the valence local orbitals of linear Be_6 are shown: there are five doubly occupied valence bonding orbitals, together with the corresponding empty antibonding orbitals. Between these two sets, two singly occupied edge orbitals are found. They come from the linear combinations of the σ_g and σ_u quasi-degenerate orbitals that are located at the Fermi level of the system.

In Figure 2b, RHF valence orbitals are shown for the cyclic (Be_6) chain at its equilibrium

geometry. In Figure 4, the corresponding local orbitals are illustrated. In this case, there are N sets of orbitals that are equivalent because of symmetry reasons. Therefore, only four types of different valence orbitals are found: bonding and antibonding, both having a σ character, as well as in-plane (σ) and out-of-plane (π) non-bonding orbitals. For this reason, only one doubly occupied bonding orbitals and its corresponding empty antibonding orbital have been reported. The in-plane non-bonding orbital is also illustrated in the figure.

In Figure 2, the orbital energies of the valence doubly occupied or singly occupied edge orbitals are also reported. For both linear and cyclic chains, the highest occupied orbitals have negative energies. In the linear Be_6 chain, the SOMO energies are closed to the highest doubly occupied orbital one.

HOMO-LUMO Energy Gap

Although the HF calculations lack the correlation contribution, the HOMO-LUMO energy gap computed at HF level is an indicator of the metallic character of an extended system. For linear chains, HOMO correspond to the highest SOMO (the two SOMO become quasi-degenerate for N $>$ 8). In Figure 5 (see also Table 1), the HOMO-LUMO gap is illustrated as a function of N for the two types of geometries. In both cases, the gap is roughly constant as a function of the system size, and no sign of metallicity is shown. The linear gap is almost constant as a function of the size, and converges toward a limit close to 0.26 *hartree* for long chains. As discussed previously, the cyclic gap shows an alternating behavior between even and odd structures. Because of this oscillating trend, its large-size limit is more difficult to evaluate, but should be close to 0.23 *hartree*. The difference between the two limit values are clearly due to the presence of the edge orbitals in the linear systems. In both cases, these results are consistent with an infinite limit of the gap well different from zero. For a comparison, the gap is 0.344943 *hartree* for the isolated Be atom, and becomes 0.260674

hartree for Be_4. In the case of Be_{13}, the gap goes down to 0.136318 (0.170492) *hartree* for the HCP (FCC) symmetry structure of the closed-shell neutral (dianion) compound. Although the comparison between gaps of systems having different charges should be taken with some caution, these values show a clear descending trend as a function of the system size, as one would expect from a metallic system.

Optimized Geometries and Harmonic Frequencies

In Tables S1 and S2, the optimized bond lengths are reported for the linear and cyclic structures, respectively. All bond distances of chain structures are systematically shorter than the value in the bulk, which is about 4.195 bohr.[37] This fact can be understood if we consider that each electron is shared among a much large number of "bonds" in the bulk than in the chains. From these tables, it appears also that the bond lengths are weakly correlated with the position of the bond, or the chain length. The terminal bonds of open chains are an exception to this behavior, since their length are considerably longer than all the other bonds. It is interesting to see that the same type of phenomenon has been described in crystalline beryllium, where the inter-planar spacing between the first and the second planes at the (0001) crystal surface has been found to be expanded by about 0.2 bohr.[38]

In cyclic Be_N, all the bonds are equivalent. The optimized bond length are reported in Table S2 and Figure 6. For small systems, the values of even cyclic chains are significantly shorter than those corresponding to odd chains. The bond lengths decreases when N increases for odd values of N and, on the contrary, increases for even N in the case of the short chains (up to $N = 7$). This can be related to the different behavior of even and odd closed chains, as discussed in the previous section. For larger values of N, on the other hand, the two curves are barely distinguishable, and they tend to the common limit of an infinite system for large values of N. The asymptotic value can be estimated to be about 4.04 bohr.

In Table S1 and Figure 7 the distances for linear chains are reported. In our notation the numbering of the bonds begins from the center and ends at the edge of the chain. Figure 7 gives a clear depiction of the general trend in bond lengths, where each curve describes an N membered chain ($N = 3, 4, ..., 12$). The external bond ($(N-1)/2$ bond number for odd systems and $N/2$ for even ones) has a value of about 4.087 bohr. In each chain, this bond is the longest one, being about 0.056 bohr longer than the previous one ($(N-3)/2$ for odd chains and $N/2-1$ for even ones). We note that the outer Be atoms are surrounded by three valence electrons compared to four electrons for the inner atoms, explaining the relatively long external bonds. The preceding ($(N-3)/2$ for odd chains and $N/2-1$ for even ones) bond is the shortest one in each chain, reaching around 4.031 bohr. Then, after slight increments in bond lengths, saturation is reached at a value $\sim$ 4.044 bohr. We note that bond lengths in chains of different sizes are reduced for the shorter chains, with the exception of Be_3. Finally, we notice that consecutive odd ($N+1$) and even (N) chains have very similar bond lengths when N increases.

It was found that the linear geometry is the most stable one only in the case of Be_4.

Concerning the linear chains, we computed harmonic frequencies at CAS(2/2) level, for the singlet and triplet states for short chains. It turns out that singlet and triplet have extremely close frequencies in the case of long chains, since these two states are almost degenerate. In other words, this means that the singlet-triplet quasi degeneracy is not removed by small bending (or stretching) of the system. For this reason, we report in this work only the frequencies for the triplet state computed at the RHF level (Table S5). The harmonic frequencies for the cyclic chains have been calculated for the RHF singlet state (Table S6). All the second derivatives where found to be positive (*i.e.*, all the harmonic frequencies are real and positive). This means that, in principle, it should be possible to produce these

molecular species, although their stability is also related to dynamical and thermodynamical aspects. The lowest bending and stretching frequencies vanish asymptotically with the number of atoms N, whereas the highest frequencies approach finite values. CCSD harmonic frequencies have also been calculated for both linear and cyclic chains, until N=8. The results, presented in Table S7 and S8, do not change significantly compared to the ones obtained at the RHF level . Indeed, the difference is no more than ± 35 cm^{-1} except for the Be_4 cyclic chain for which one frequency is found 129 cm^{-1} lower at the correlated level (344.73 cm^{-1} compared to 481.05 cm^{-1}).

Extrapolated Energies

The total CCSD(T) energies can be found in Tables S3 and S4 while the per-atom CCSD(T) energies are plotted in Figure 8 as a function of $1/N$ (linear clusters), and $1/N^2$ (cyclic clusters). For sake of comparison, the energies for Be, Be_4, Be_{13} are given in Table 2. In the case of cyclic structures, the odd values on N show a behavior that is slightly different from the even values, as discussed earlier, the curves shown in the figure have a remarkably linear character for the largest values of N. By interpolating the energies corresponding to the last seven values (N=6,...,12) we obtain a behavior given by

$$E_{\rm lin}(N)/N \;=\; -14.658 + 0.1044\frac{1}{N} \tag{4}$$

and

$$E_{\rm cyc}(N)/N \;=\; -14.658 + 0.4334\frac{1}{N^2} \tag{5}$$

The intercept at the abscissa equal to zero of these straight lines corresponds to the limit for $N \to \infty$ of the energy per monomer. The fact that the values obtained from the two different types of systems are coincident within a *mhartree* confirms the consistency of the model. It is also a further indication of the strong covalent nature of the bonds, since the absence of size effects (except $N = 3$ and $N = 4$ for the cyclic case) indicates the absence of

any remarkable sign of electron delocalization.

As already anticipated, the odd cyclic chains have a behavior that is slightly different from the even chain ones. In particular, the points lies on a straight line to a worse approximation (this is illustrated in Figure 8). Although this is hardly surprising in the case $N = 3$, since the strain angle is in this case very large, the behavior is much more surprising in the case $N = 5$. In fact, this point is less well described by a linear fitting in $1/n^2$ than the even chain $N = 4$, which in principle has a much larger strain. We should also mention the fact that linear chains studied in previous works[17] showed effects somehow reminding the present one: in particular, we remarked a parity effect in both the ST splitting in neutral chains and in the interaction in cationic or anionic bistable chains.

This alternating behavior is found also by looking at the equilibrium bond lengths of the cyclic forms, reported in Table S2 and Figure 6 and already discussed.

The Total-Position Spread Tensor

The TPS tensor gives useful information about the metallicity of the system. The isolated atomic value is $\Lambda = 3.9491\ bohr^2$, while the tetrahedral Be_4 has the three degenerate components equal to $\Lambda = 24.1284\ bohr^2$, which gives a per-atom value of $\Lambda = 6.0321\ bohr^2$. This trend is consistent with the well known metallic nature of bulk beryllium.

The chain values are reported in Tables 3 (cyclic) and 4 (linear), and illustrated in Figures 9, 10, and 11. We computed both the spin-summed quantities and the spin-partitioned $\alpha\alpha + \beta\beta$ and $\alpha\beta + \beta\alpha$ ones. For a single Slater determinant, the $\alpha\beta + \beta\alpha$ term is zero for the cyclic case, and therefore only the spin-summed component is shown. For linear chains, $\Lambda_{\parallel}$ indicates the component in the chain direction, while $\Lambda_{\perp}$ are the doubly degenerate components in the directions orthogonal to the chain. For cyclic chains, on the other hand, $\Lambda_{\parallel}$

indicates the doubly degenerate components that lie on the chain plane, while $\Lambda_\perp$ is the component in the direction orthogonal to this plane. Both singlet and triplet values were reported for the linear case. Singlet and triplet spreads, however, are almost coincident but for the shortest chains, since the corresponding wavefunctions are almost identical, except for the spin coupling of the electrons in the singly occupied orbitals.

In all cases, the spin-summed values become quickly proportional to the number of atoms, as shown in Figures 9a and 10a. Moreover, from Figures 9b and 10b it appears that Λ/N converges to a constant value *from above*, thus excluding the possibility of a slow divergence of this quantity. This is a clear indication of the non-metallic nature of the chains. As expected, the cyclic chains saturate more rapidly than the linear ones, because of the border effects that are present in the latter. In particular, the orthogonal components $\Lambda_\perp/N$ for both cyclic and linear systems converge toward a common limit that is close to 4.2 $bohr^2$. Remarkably, the parallel components are even *smaller* than the perpendicular ones, showing a very little mobility of the electrons in the directions of the chains. These components have obviously different behaviors for the linear and cyclic systems, since the spread is purely longitudinal in the former case, and a mixture of longitudinal and transversal spread in the latter case. However, in the case of a local character of the spread and because of its quadratic nature as a function of the coordinates, one would expect that $\Lambda_\parallel/N$ for the cyclic systems is close to the average between $\Lambda_\parallel/N$ and $\Lambda_\perp/N$ for the linear case. This is indeed the case, with $\Lambda_\parallel/N = 3.9$ $bohr^2$ for the cycles, while $\Lambda_\perp/N = 4.2$ $bohr^2$ and $\Lambda_\parallel/N = 3.5$ $bohr^2$ for the linear geometries (average value: 3.9 $bohr^2$). This is slightly above the atomic spread (3.9491), but well below the per-atom Be_4 value for the cluster with T_d symmetry (6.0321).

The *per electron* eigenvalues of the spread tensor for both types of chains quickly saturate for large structures (actually, they even show a tiny reduction of their magnitude). These facts clearly indicate, in our opinion, that quasi-1D beryllium systems do not have a *metallic*

nature. On the contrary, we believe that they can be seen as prototypes of 1D *covalent* chains.

Spread data for FCC Be_{13}, admit a less clear interpretation, because of the ionic character of the wave function. The spread for the Be_{13}^{+} cluster is obviously much less than the one for Be_{13}^{2-}, partly because of the slightly larger bond lengths and the presence of three more electrons in the latter, but in particular for the more diffuse nature of the anionic wave function with respect to the cationic one. The per-atom values are comprised between 5.5561 for Be_{13}^{+} and 7.1731 for Be_{13}^{2-}. HCP Be_{13} has values 5.9775 for the axial component and 6.0953 for the two degenerate equatorial components. It is clear from these results that the longitudinal components of the TPS in quasi-1D structures do not show any signature of a metallic nature of the wave function, contrary to what happens for the 3D case.

Conclusions

A theoretical Coupled-Cluster study on the equilibrium geometry and harmonic frequencies of quasi-1D beryllium structures, having either linear or cyclic geometries, was reported. It was shown that the effect of dynamical correlation do not significantly change the HF results. In conclusion, quasi-1D Be_N systems are likely to be metastable clusters.

The equilibrium bond lengths of the studied systems are weakly dependent on the size of the chain or the position of the bond along the chain. Moreover, harmonic frequencies, computed at CCSD level, are in good agreement with previous CAS-SCF computations.

The reported calculations give information about the nature of the ground states of beryllium linear structures. All the indicators point toward a non-metallic, covalent type of bond between neighbor atoms. In particular, we found a HOMO-LUMO gap larger than 6 eV for the biggest clusters, there is no tendency to shrink as the size of the system increases. The valence Molecular Orbitals of the chains can be well localized, and they correspond to

bond orbitals located on pairs of neighbor atoms, contrary to what happens in the case of metallic structures. Finally, what is probably the strongest evidence of a non-metallic nature of the systems is the fact that the TPS tensor has a linear dependence on the system size.

According to our results, both linear and cyclic structures are local minima on the corresponding PES. For a given value of N, the cyclic structures are more stable than the linear ones, except in the case of Be_4. Nevertheless, more compact (i.e., 3D) clusters are much more stable, with total energies considerably lower. The possible existence of these clusters in quasi-1D geometries depend on the barrier toward more stable arrangements. Transition states connecting these minima should be investigated to conclude.

Acknowledgement

This work was partly supported by the French "Centre National de la Recherche Scientifique" (CNRS, also under the PICS action 4263). It has received fundings from the European Union's Horizon 2020 research and innovation programme under the Marie Skłodowska-Curie grant agreement n°642294. This work was also supported by the Programme Investissements d'Avenir under the program ANR-11-IDEX-0002-02, reference ANR-10-LABX-0037-NEXT. The calculations of this work have been partly performed by using the resources of the HPC center CALMIP under the grant 2016-p1048. One of us (AWH) acknowledges the support of the "Theoretical Chemistry and Computational Modeling" (TCCM) Erasmus-Plus Master program. Finally, we would like to thank Ulf Saalman (Max-Planck-Institut für Physik komplexer Systeme, Dresden), for interesting discussion and suggestions.

Supporting Information Available

The document `SI-Be.pdf` contains:

- Table S1: CCSD equilibrium bond distances as a function of the chain length N for the linear chains.
- Table S2: CCSD equilibrium bond distances as a function of the chain length N for the cyclic chains.
- Table S3: Total energies for cyclic Be_N clusters (singlet ground state).
- Table S4: Total energies for linear Be_N clusters (lowest triplet state).
- Table S5: RHF Harmonic frequencies of the normal modes for linear Be_N, for $N = 3, 4, ..., 12$.
- Table S6: RHF Harmonic frequencies of the normal modes for cyclic Be_N, for $N = 3, 4, ..., 12$.
- Table S7: CCSD Harmonic frequencies of the normal modes for linear Be_N, for $N = 3, 4, ..., 8$.
- Table S8: CCSD Harmonic frequencies of the normal modes for cyclic Be_N, for $N = 3, 4, ..., 8$.

This material is available free of charge via the Internet at `http://pubs.acs.org/`.

References

(1) Emberly, E. G.; Kirczenow, G. Electron standing-wave formation in atomic wires. *Phys. Rev. B* **1999**, *60*, 6028–6033.

(2) Bahn, S. R.; Jacobsen, K. W. Chain formation of metal atoms. *Phys. Rev. Lett.* **2001**, *87*, 266101.

(3) Himpsel, F. J.; Altmann, K. N.; Bennewitz, R.; Crain, J. N.; Kirakosian, A.; Lin, J.-L.; McChesney, J. L. One-dimensional electronic states at surfaces. *J. Phys.: Cond. Matt.* **2001**, *13*, 11097–11113.

(4) Amorim, E. P. M.; Silva, A. J. R. d.; Fazzio, A.; Silva, E. Z. d. Short linear atomic chains in copper nanowires. *Nanotechnology* **2007**, *18*, 145701.

(5) Crain, J. N. End states in one-dimensional atom chains. *Science* **2005**, *307*, 703–706.

(6) Davison, S. G.; Stlicka, M. *Basic Theory of Surface States*, reprinted ed.; Monographs on the physics and chemistry of materials 46; Clarendon Press, 2008; OCLC: 553640577.

(7) Hod, O.; Peralta, J. E.; Scuseria, G. E. Edge effects in finite elongated graphene nanoribbons. *Phys. Rev. B* **2007**, *76*, 233401.

(8) Hod, O.; Barone, V.; Scuseria, G. E. Half-metallic graphene nanodots: A comprehensive first-principles theoretical study. *Phys. Rev. B* **2008**, *77*, 035411.

(9) Son, Y.-W.; Cohen, M. L.; Louie, S. G. Half-metallic graphene nanoribbons. *Nature* **2006**, *444*, 347–349.

(10) Vetere, V.; Monari, A.; Scemama, A.; Bendazzoli, G. L.; Evangelisti, S. A theoretical study of linear beryllium chains: full configuration interaction. *J. Chem. Phys.* **2009**, *130*, 024301.

(11) Yáñez, M.; Sanz, P.; Mó, O.; Alkorta, I.; Elguero, J. Beryllium bonds, do they exist? *J. Chem. Theory Comput.* **2009**, *5*, 2763–2771.

(12) Mó, O.; Yáñez, M.; Alkorta, I.; Elguero, J. Modulating the strength of hydrogen bonds through beryllium bonds. *J. Chem. Theory Comput.* **2012**, *8*, 2293–2300.

(13) Brea, O.; Alkorta, I.; Mó, O.; Yáñez, M.; Elguero, J.; Corral, I. Exergonic and spontaneous production of radicals through beryllium bonds. *Angew. Chem.* **2016**, *128*, 8878–8881.

(14) Brea, O.; Corral, I.; Mó, O.; Yáñez, M.; Alkorta, I.; Elguero, J. Beryllium-based anion sponges: close relatives of proton sponges. *Chem. - Eur. J.* **2016**, *22*, 18322–18325.

(15) Montero-Campillo, M. M.; Corral, I.; Mó, O.; Yáñez, M.; Alkorta, I.; Elguero, J. Beryllium-based fluorenes as efficient anion sponges. *Phys. Chem. Chem. Phys.* **2017**, *19*, 23052–23059.

(16) Brea, O.; Mó, O.; Yáñez, M.; Alkorta, I.; Elguero, J. On the existence of intramolecular one-electron Be–Be bonds. *Chem. Commun.* **2016**, *52*, 9656–9659.

(17) Monari, A.; Bendazzoli, G. L.; Evangelisti, S. Theoretical study of Be_N linear chains: optimized geometries and harmonic Frequencies. *J. Chem. Theory Comput.* **2009**, *5*, 1266–1273.

(18) Helal, W.; Monari, A.; Evangelisti, S.; Leininger, T. Electronic bistability in linear beryllium chains. *J. Phys. Chem. A* **2009**, *113*, 5240–5245.

(19) Pastore, M.; Monari, A.; Angeli, C.; Bendazzoli, G. L.; Cimiraglia, R.; Evangelisti, S. A theoretical study of Be_N linear chains: variational and perturbative approaches. *J. Chem. Phys.* **2009**, *131*, 034309.

(20) Pastore, M.; Monari, A.; Evangelisti, S.; Leininger, T. Mixed valence character of anionic linear beryllium chains: a CAS-SCF and MR-CI study. *J. Phys. Chem. A* **2009**, *113*, 14706–14710.

(21) Evangelisti, S.; Monari, A.; Leininger, T.; Bendazzoli, G. L. Beryllium chains interacting with graphene nanoislands: from anti-ferromagnetic to ferromagnetic ground state. *Chem. Phys. Lett.* **2010**, *496*, 306–309.

(22) Tague, T. J.; Andrews, L. Reactions of beryllium atoms with hydrogen. Matrix infrared spectra of novel product molecules. *J. Am. Chem. Soc."* **1993**, *115*, 12111–12116.

(23) Fertitta, E.; Paulus, B.; Barcza, G.; Legeza, Ö. Investigation of metal–insulator-like transition through the *ab initio* density matrix renormalization group approach. *Phys. Rev. B* **2014**, *90*, 245129.

(24) Fertitta, E.; Paulus, B.; Barcza, G.; Legeza, Ö. On the calculation of complete dissociation curves of closed-shell pseudo-onedimensional systems via the complete active space method of increments. *J. Chem. Phys.* **2015**, *143*, 114108.

(25) Koch, D.; Fertitta, E.; Paulus, B. Calculation of the static and dynamical correlation energy of pseudo-one-dimensional beryllium systems via a many-body expansion. *J. Chem. Phys.* **2016**, *145*, 024104.

(26) Bendazzoli, G. L.; Evangelisti, S.; Monari, A.; Paulus, B.; Vetere, V. Full configuration-interaction study of the metal-insulator transition in model systems. *J. Phys.: Conf. Ser.* **2008**, *117*, 012005.

(27) Resta, R.; Sorella, S. Electron localization in the insulating state. *Phys. Rev. Lett.* **1999**, *82*, 370–373.

(28) Resta, R. Why are insulators insulating and metals conducting? *J. Phys.: Condens. Matter* **2002**, *14*, R625.

(29) Resta, R. Kohns theory of the insulating state: A quantum-chemistry viewpoint. *J. Chem. Phys.* **2006**, *124*, 104104.

(30) Resta, R. Polarization Fluctuations in Insulators and Metals: New and Old Theories Merge. *Phys. Rev. Lett.* **2006**, *96*, 137601.

(31) Widmark, P.-O.; Malmqvist, P.-Å.; Roos, B. O. Density matrix averaged atomic natural orbital (ANO) basis sets for correlated molecular wave functions: I. First row atoms. *Theor. Chim. Acta* **1990**, *77*, 291–306.

(32) Werner, H.-J. et al. *MOLPRO, version 2015.1, a package of ab initio programs*; 2015.

(33) Hampel, C.; Peterson, K. A.; Werner, H.-J. A comparison of the efficiency and accuracy of the quadratic configuration interaction (QCISD), coupled cluster (CCSD), and Brueckner coupled cluster (BCCD) methods. *Chem. Phys. Lett.* **1992**, *190*, 1–12.

(34) Watts, J. D.; Gauss, J.; Bartlett, R. J. Coupled–cluster methods with noniterative triple excitations for restricted open–shell Hartree–Fock and other general single determinant reference functions. Energies and analytical gradients. *J. Chem. Phys.* **1993**, *98*, 8718–8733.

(35) Eckert, F.; Pulay, P.; Werner, H.-J. Ab initio geometry optimization for large molecules. *J. Comput. Chem.* **1997**, *18*, 1473–1483.

(36) Maynau, D.; Evangelisti, S.; Guihéry, N.; Calzado, C. J.; Malrieu, J.-P. Direct generation of local orbitals for multireference treatment and subsequent uses for the calculation of the correlation energy. *J. Chem. Phys.* **2002**, *116*, 10060.

(37) Kittel, C. *Introduction to solid state physics*, 8th ed.; John Wiley & Sons, Inc, 2004.

(38) Davis, H. L.; Hannon, J. B.; Ray, K. B.; Plummer, E. W. Anomalous interplanar expansion at the (0001) surface of Be. *Physical Review Letters* **1992**, *68*, 2632–2635.

Table 1: HOMO-LUMO energy gap obtained by ROHF/RHF calculations for the linear and cyclic structures. Energy values are in hartree.

N	linear	cyclic
3	0.260950	0.250322
4	0.260679	0.212153
5	0.260644	0.235867
6	0.260686	0.217744
7	0.260904	0.233666
8	0.261172	0.222158
9	0.261512	0.232881
10	0.261825	0.225006
11	0.262146	0.232277
12	0.262413	0.226369

Table 2: Total energies for the singlet ground state of the isolated Be atom and three 3-D clusters (Be_4, Be_{13} FCC and Be_{13} HCP). For Be_{13} FCC two undistorted clusters have been studied: the high-spin (quartet) Be_{13}^{+} and the closed-shell Be_{13}^{2-}. For Be_{13} HCP the triplet with an "ideal" geometry has been considered. Energies are in hartree.

system	RCCSD(T)	RCCSD	RHF-SCF
Be	-14.61896573	-14.61896573	-14.57298670
Be_4	-58.60931559	-58.58345127	-58.35870626
FCC Be_{13}^{+}	-190.62705587	-190.52910207	-189.76368163
FCC Be_{13}^{2-}	-190.93162621	-190.81969066	-189.96562397
HCP Be_{13}	-190.76001277	-190.65777865	-189.85624311

Table 3: TPS tensor for cyclic Be_N clusters. The isolated Be atom value is 3.949061 $bohr^2$, while the Be_4 value for the cluster with T_d symmetry is 24.128468. For the FCC clusters with I_h symmetry, the TPS value is 72.229108 for Be_{13}^{+} and 93.249672 for Be_{13}^{2-}, while the HCP Be_{13} has values 77.705190 (the axial component) and 79.392777 (the two degenerate equatorial components). All TPS values are in $bohr^2$.

N	$\Lambda_{\parallel}$	$\Lambda_{\perp}$
3	22.40055271	14.61175820
4	20.10512254	17.33366066
5	24.19144676	21.57474198
6	26.26399922	25.42874598
7	29.76517495	29.56328841
8	32.95341909	33.63912437
9	36.48514744	37.77095934
10	39.98501422	41.89523029
11	43.58183491	46.03325189
12	47.19360128	50.17274976

Table 4: TPS tensor for linear Be_N clusters.

N	${}^3\Sigma_u\ \Lambda_\parallel$	${}^3\Sigma_u\ \Lambda_\perp$	${}^1\Sigma_g\ \Lambda_\parallel$	${}^1\Sigma_g\ \Lambda_\perp$	${}^1\Sigma_g\ \Lambda_\parallel^{\alpha\alpha+\beta\beta}$	${}^1\Sigma_g\ \Lambda_\parallel^{\alpha\beta+\beta\alpha}$
3	11.36190259	13.24719585	12.25496116	13.36032816	66.51043287	-54.25547170
4	15.00274761	17.45137526	15.24779377	17.47028013	122.41199734	-107.16420357
5	18.51186839	21.62742504	18.56716211	21.63077807	193.68876105	-175.12159893
6	21.96918759	25.79452283	21.98197352	25.79502058	281.08133953	-259.09936600
7	25.40448964	29.95848755	25.40676696	29.95858478	384.79795293	-359.39118597
8	28.82989461	34.12105801	28.83050954	34.12106795	504.88414711	-476.05363756
9	32.25083491	38.28292822	32.25088095	38.28293151	641.34745876	-609.09657781
10	35.66977175	42.44445216	35.66981185	42.44445205	794.18957727	-758.51976542
11	39.08783634	46.60574585	39.08783014	46.60574593	963.40895434	-924.32112419
12	42.50563131	50.76689007	42.50563579	50.76688997	1149.00329929	-1106.49766350

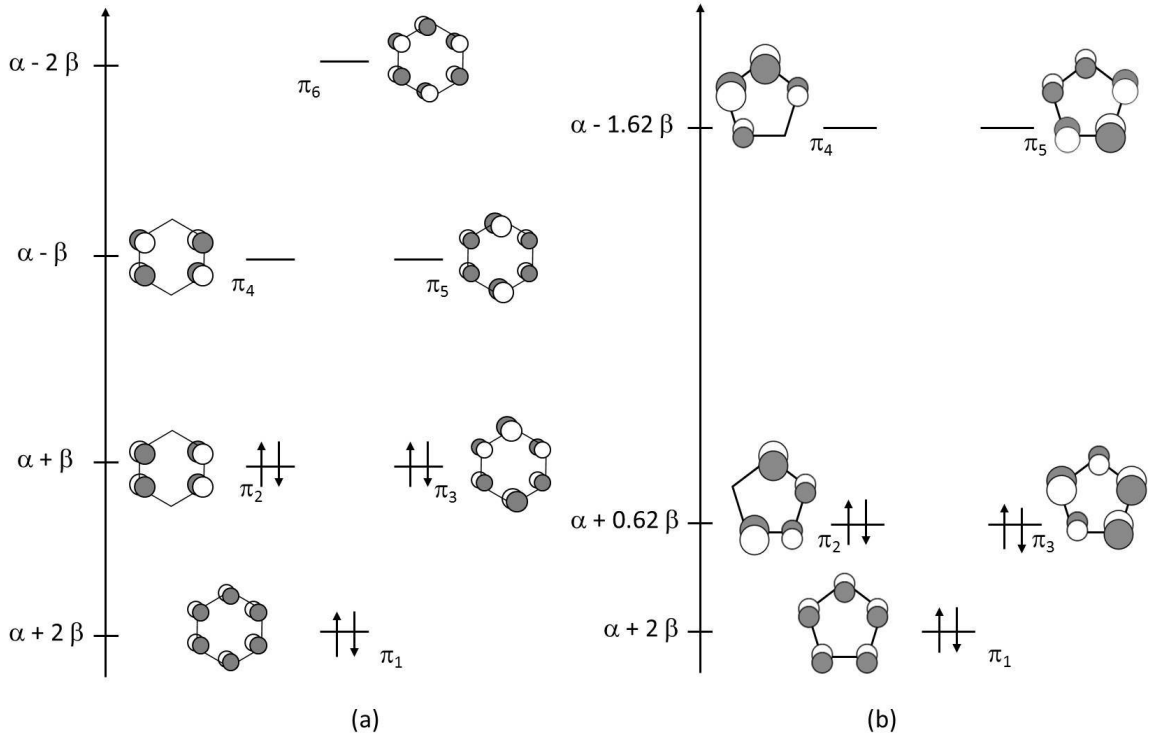

Figure 1: The Hückel π Molecular Orbitals of (a) benzene C_6H_6 and (b) cyclopentadienyl anion C_5H_5. Orbital energies are given as a function of the Hückel parameters α and β.

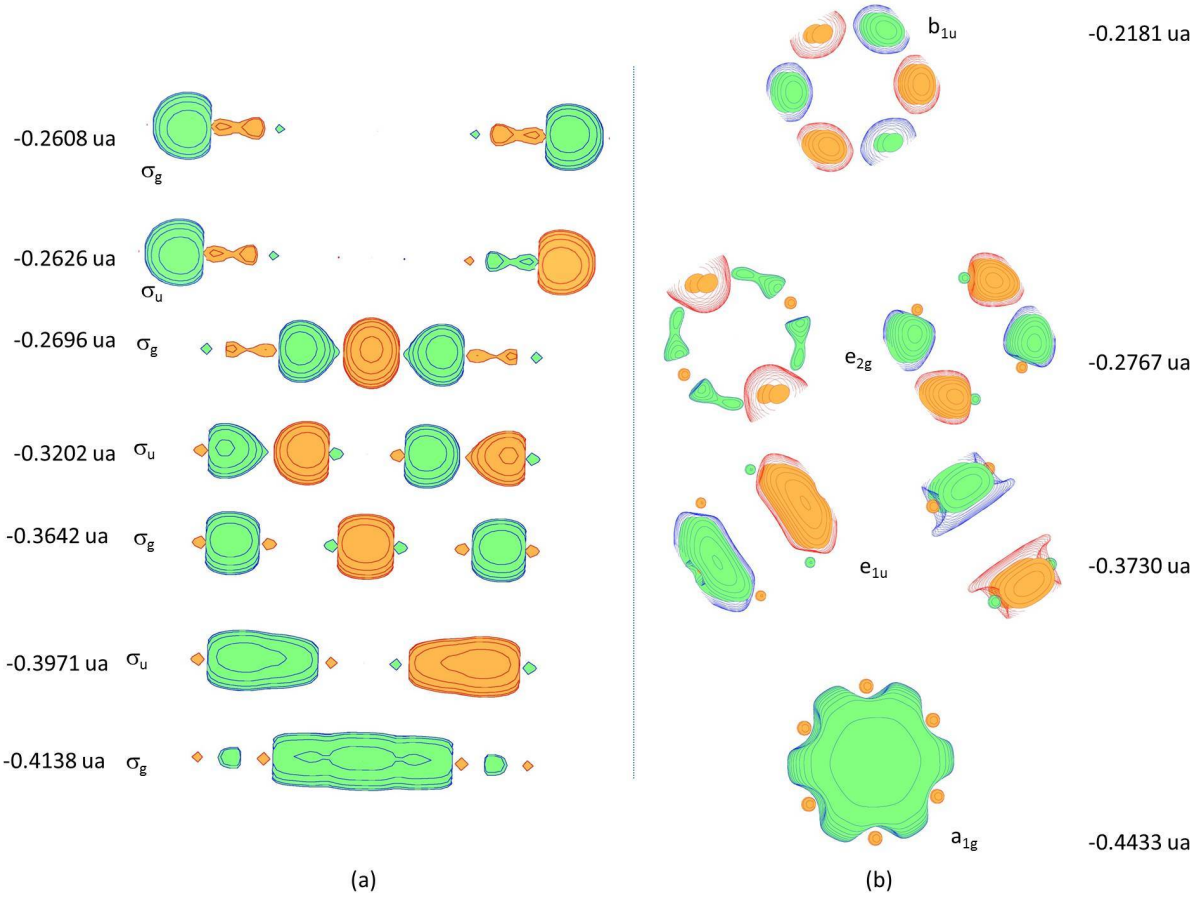

Figure 2: Canonical Occupied Molecular Orbitals (MO) of (a) Linear Be_6 ($D_{\infty h}$) computed at ROHF level and (b) Cyclic Be_6 (D_{Nh}) computed at RHF level. The MO symmetries are specified and the orbital energies are given (*hartree*).

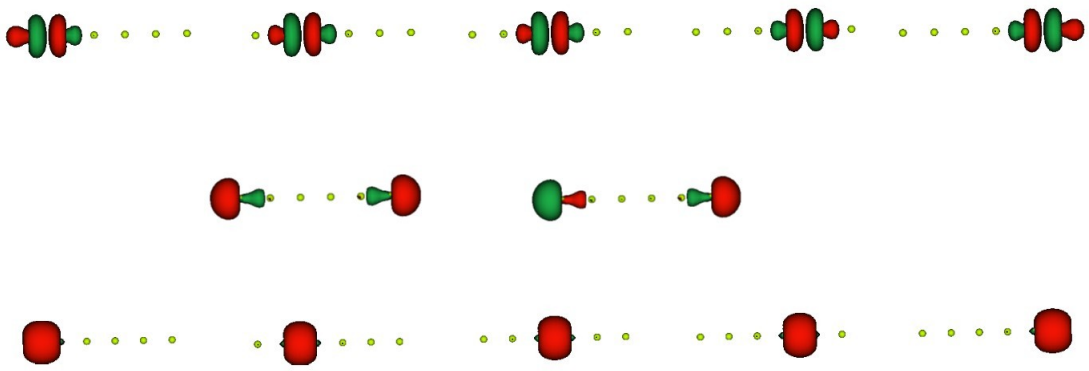

Figure 3: The 12 valence orbitals having σ character of the Be_6 chain, local picture: the five occupied bonding orbitals (bottom); the two singly occupied edge orbitals (middle); the five empty virtual orbitals (top). The π orbitals are not shown.

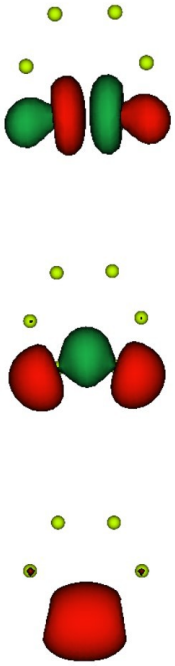

Figure 4: Three out of the 18 valence orbitals having σ character of cyclic Be_6, local picture: a bonding occupied orbital (bottom); an empty non-bonding orbital (middle); an empty virtual orbital (top). The remaining 15 σ orbitals are equivalent by symmetry to these three ones by rotation around the C_6 axis. The π orbitals are not shown.

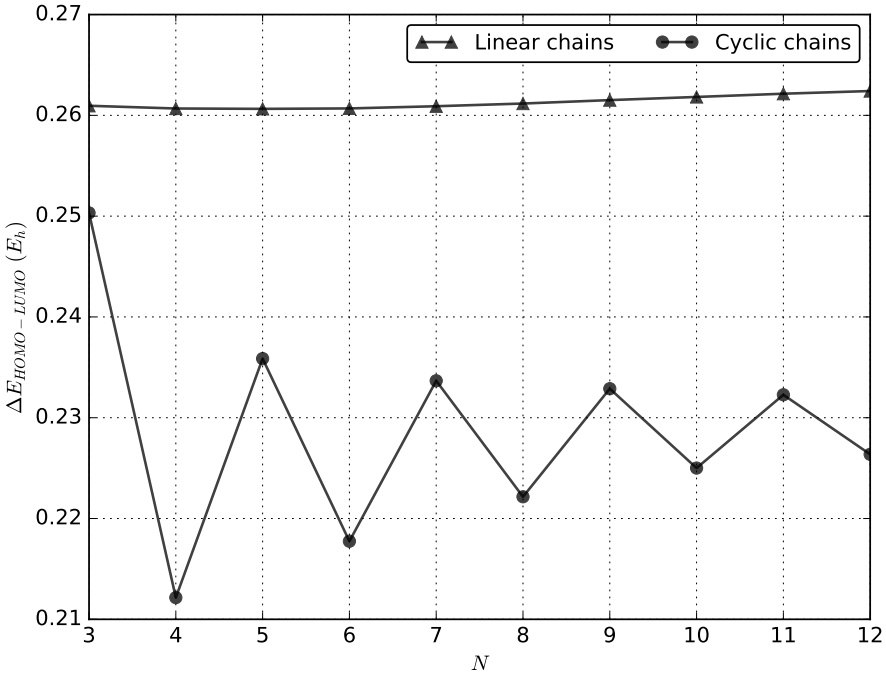

Figure 5: The HOMO-LUMO energy gap obtained by ROHF/RHF calculations for both type of chains, as a function of the number of beryllium atoms N. Energies in *hartree*.

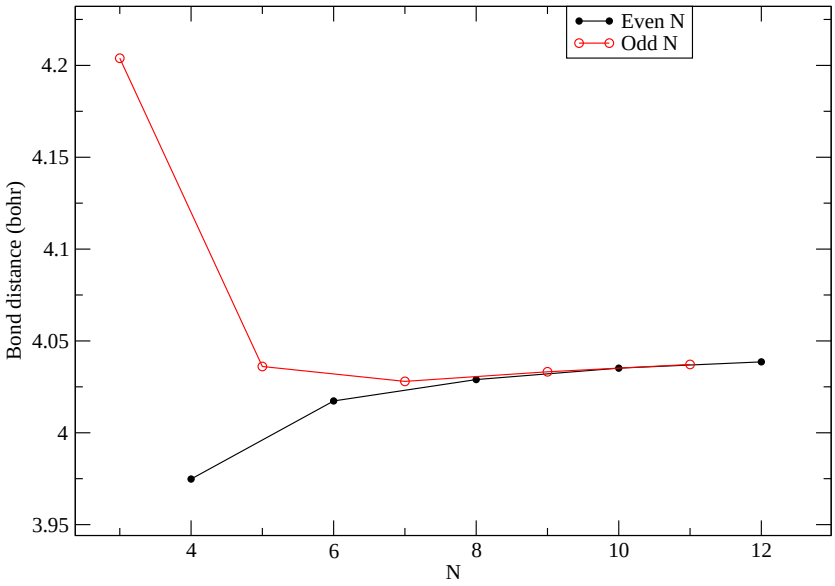

Figure 6: The optimized CCSD bond lengths (*bohr*) as a function of the number of Be atoms (N), for cyclic Be_N, N=3,...,12.

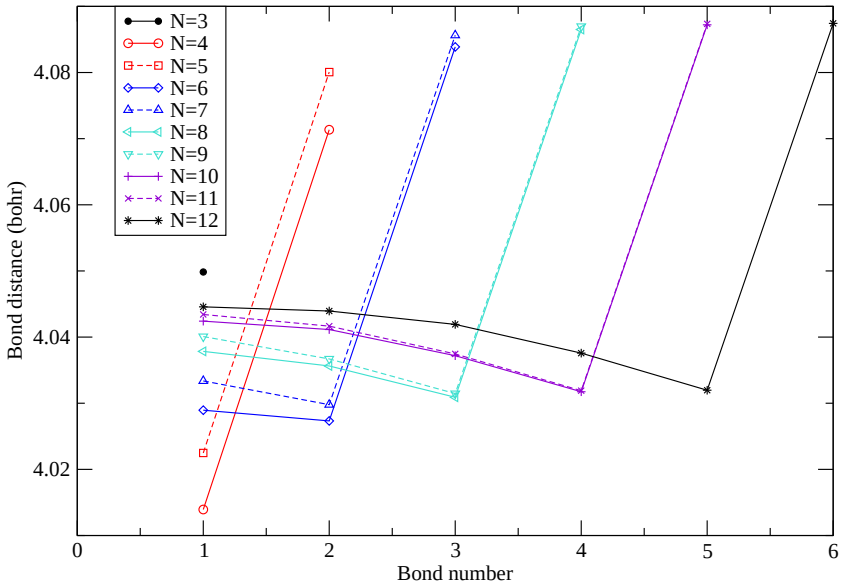

Figure 7: The optimized CCSD bond lengths (*bohr*) as a function of the bond position in the chain, for linear Be_N, N=3,...,12.

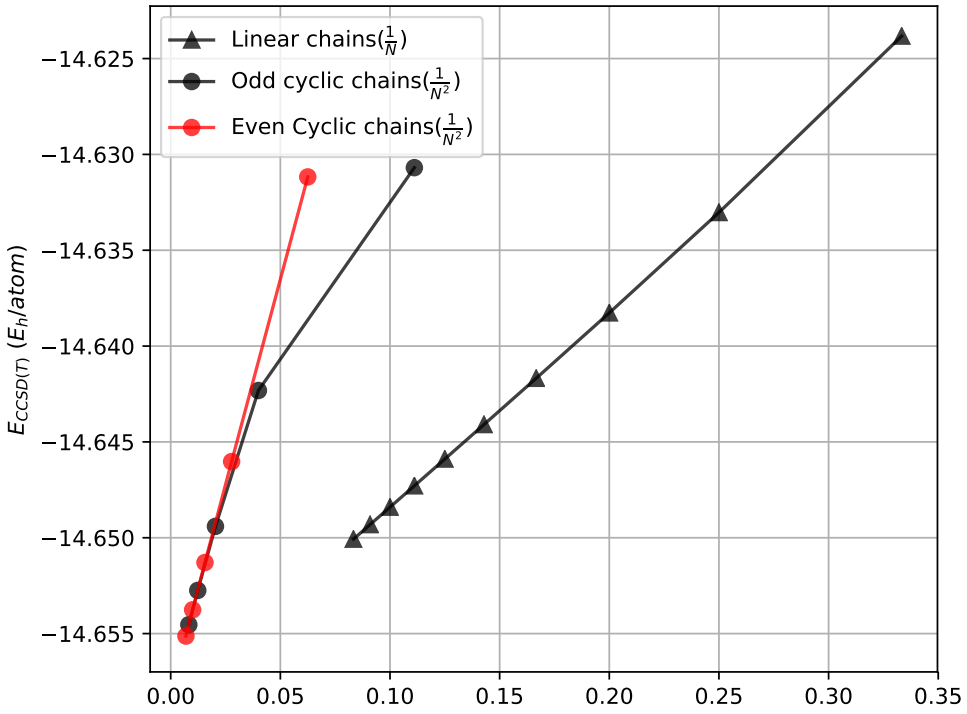

Figure 8: The CCSD(T) energies per Be atom (*hartree*), as a function of $1/N$ (linear chains) and $1/N^2$ (cyclic chains).

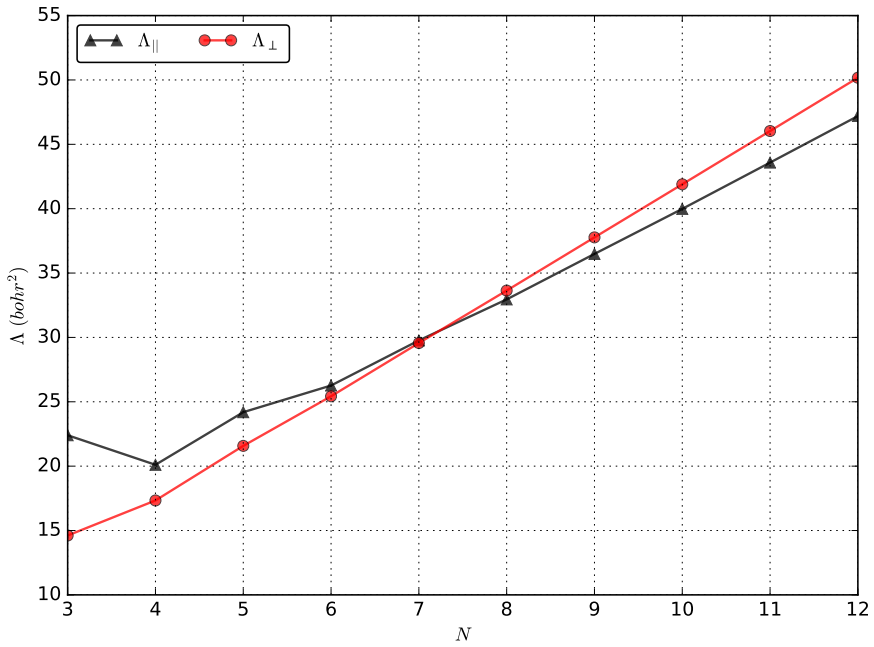

(a) The spin-summed TPS for cyclic chains: planar (degenerate) components ($\Lambda_{\parallel}$) and out-of-plane component ($\Lambda_{\perp}$). The isolated Be atom value is 3.949061, while the Be_4 value is 24.128468. All values in $bohr^2$.

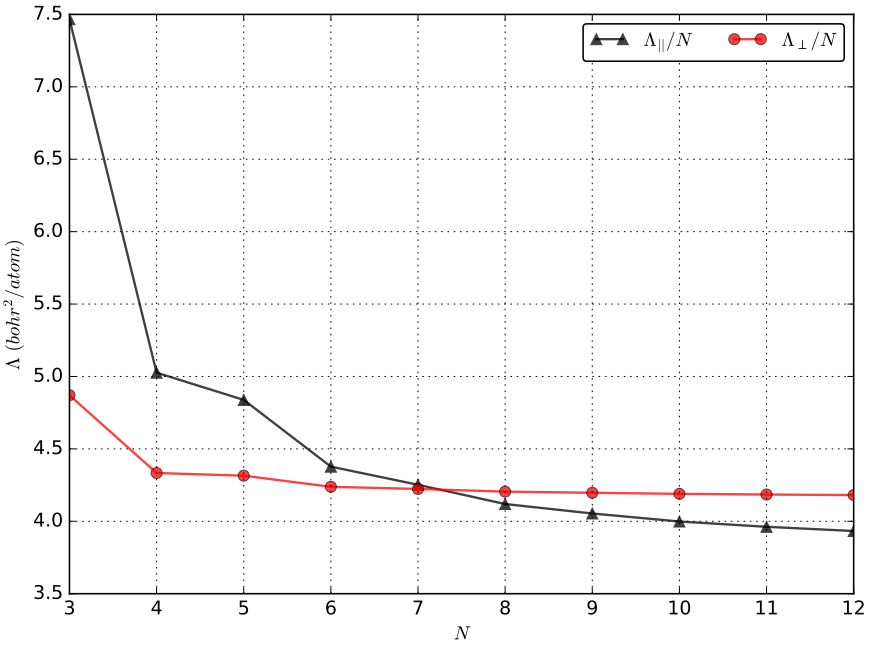

(b) The spin-summed TPS for cyclic chains, divided by the number of beryllium atoms N: planar (degenerate) components ($\Lambda_{\parallel}/N$) and out-of-plane component ($\Lambda_{\perp}/N$).

Figure 9: The spin-summed TPS for cyclic chains

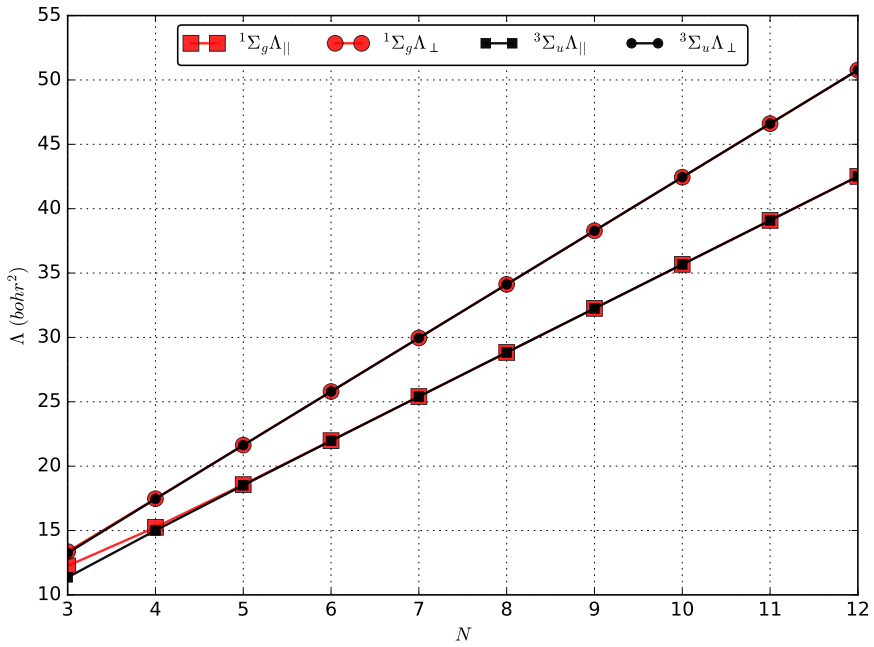

(a) The spin-summed TPS for linear chains: perpendicular (degenerate) components and parallel component. The singlet (red) and triplet (black) values are virtually degenerate for $N > 5$.

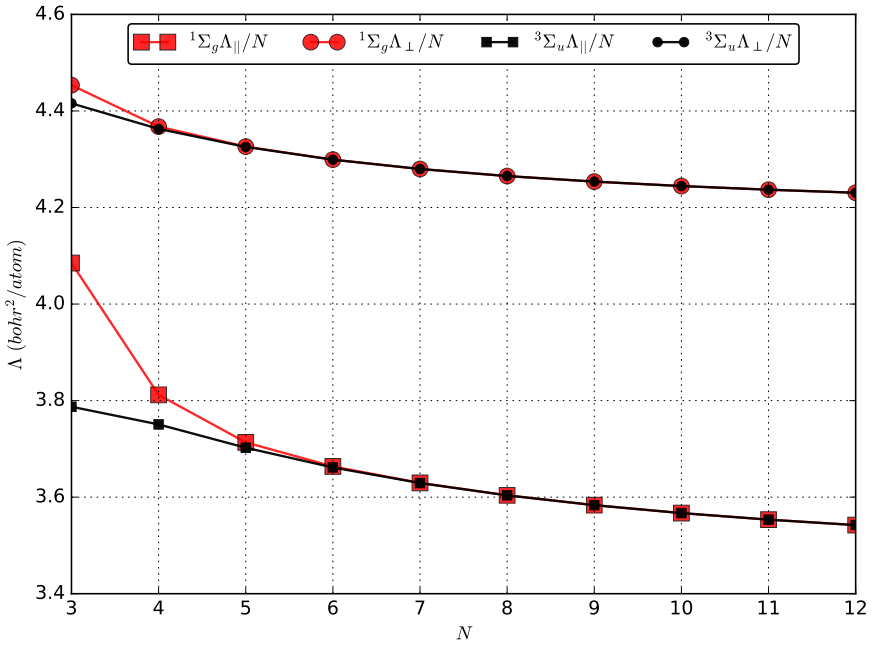

(b) The spin-summed TPS for linear chains, divided by the number of beryllium atoms N: perpendicular (degenerate) components and parallel component.

Figure 10: The spin-summed TPS for linear chains

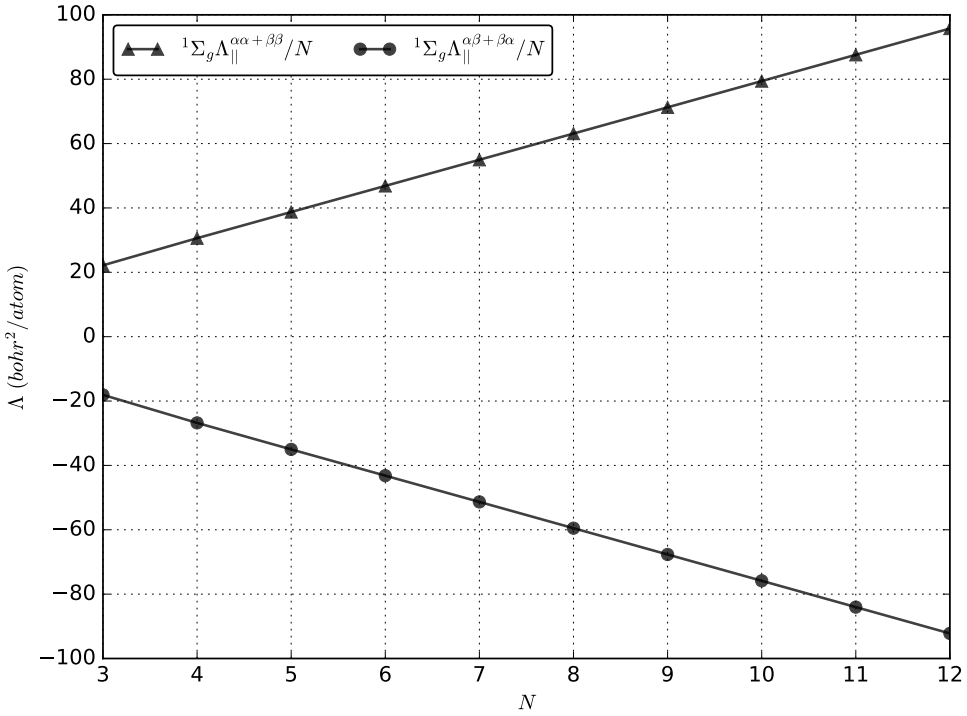

Figure 11: The spin-partitioned parallel component of the TPS tensor for linear chains, divided by the number of beryllium atoms N: the $\alpha\alpha + \beta\beta$ and $\alpha\beta + \beta\alpha$ components.

for Table of Contents use only

The Electronic Structure of Beryllium Chains

Ahmad W. Huran, Nadia Ben Amor, Stefano Evangelisti, Sophie Hoyau, Thierry Leininger, and Véronique Brumas